Published in final edited form as:
Neurogastroenterol Motil. 2007 October ; 19(10): 845–855. doi:10.1111/j.1365-2982.2007.00976.x.

α_2-ADRENOCEPTORS COUPLE TO INHIBITION OF R-TYPE CALCIUM CURRENTS IN MYENTERIC NEURONS

Xiaochun Bian and **James J. Galligan**
Department of Pharmacology and Toxicology and the Neuroscience Program, Michigan State University, East Lansing, Michigan 48824 USA

Abstract

α_2-adrenoceptors inhibit Ca^{2+} influx through voltage-gated Ca^{2+} channels throughout the nervous system and Ca^{2+} channel function is modulated following activation of some G-protein coupled receptors. We studied the specific Ca^{2+} channel inhibited following α_2-adrenoceptor activation in guinea pig small intestinal myenteric neurons. Ca^{2+} currents (I_{Ca}^{2+}) were studied using whole-cell patch clamp techniques. Changes in intracellular Ca^{2+} ($\Delta[Ca^{2+}]_i$) in nerve cell bodies and varicosities were studied using digital imaging where Ca^{2+} influx was evoked by KCl (60 mM) depolarization. The α_2-adrenoceptor agonist, UK 14,304 (0.01 − 1 μM) inhibited I_{Ca}^{2+} and $\Delta[Ca^{2+}]_i$; maximum inhibition of I_{Ca}^{2+} was 40%. UK 14,304 did not affect I_{Ca}^{2+} in the presence of SNX-482 or $NiCl_2$ (R-type Ca^{2+} channel antagonists). UK 14,304 inhibited I_{Ca}^{2+} in the presence of nifedipine, ω-agatoxin IVA or ω-conotoxin, inhibitors of L-, P/Q- and N-type Ca^{2+} channels. UK 14,304 induced Inhibition of I_{Ca}^{2+} was blocked by pertussis toxin pretreatment (1 μg/ml for 2 hr). α_2-Adrenoceptors couple to inhibition of R-type Ca^{2+} channels via a pertussis toxin-sensitive pathway in myenteric neurons. R-type channels may be a target for the inhibitory actions of norepinephrine released from sympathetic nerves on to myenteric neurons.

Keywords

α1E; $Ca_{v2.3}$; calcium imaging; enteric nervous system; presynaptic inhibition

Gastrointestinal motility is controlled in part by the enteric nervous system (ENS) and by extrinsic sympathetic nerves. The ENS provides primary control over gut function while the sympathetic innervation modulates ENS activity (1). The myenteric plexus, a division of the ENS, is particularly important for control of gastrointestinal motility (2). Using electrophysiological criteria, myenteric neurons can be classified as S or AH neurons (3) and AH neurons may be intrinsic primary afferent neurons (4). In AH neurons the action potential has a Ca^{2+} shoulder that is dependent on activation of N-type Ca^{2+} channels (5). Ca^{2+} entering during the action potential triggers calcium release from intracellular stores (6,7). The rise in intracellular Ca^{2+} then activates a Ca^{2+}-dependent K^+ channel, causing a long-lasting afterhyperpolarization (AHP)(4,8,9). S neurons are interneurons and motorneurons (10). Although action potentials in S neurons are blocked completely by tetrodotoxin (sodium channel antagonist), they are also associated with increases in intracellular calcium that are partly dependent on activation of N-type Ca^{2+} channels (11).

Guinea pig myenteric neurons express multiple Ca2+ subtypes (12). The total Ca^{2+}current (I_{Ca}^{2+}) in myenteric neurons is composed of contributions of Ca^{2+} influx through L- N- P/Q-

Correspondence: James J. Galligan, Ph.D. Department of Pharmacology and Toxicology B-328, Life Science Building Michigan State University East Lansing, MI 48823, USA Tel: 1−517−353−4776 Fax: 1−517−353−8915 Email: E-mail: galliga1@msu.edu.

and R-type Ca^{2+} channels (13-18). The R-type channels make the largest contribution to the total I_{Ca}^{2+} in myenteric neurons of guinea-pig small intestine maintained in the primary culture (13). R-type Ca^{2+} channels are composed of the pore forming α_{1E} subunit (19,20). SNX 482 (21) or low concentrations of $NiCl_2$ (13,22) can block selectively currents passing through R-type channels.

Sympathetic nerves inhibit intestinal motility by releasing norepinephrine which activates inhibitory α_2-adrenoceptors expressed by myenteric neurons and their nerve endings (24,25). α_2-Adrenoceptors couple to inhibition of calcium influx through voltage-gated calcium channels via a G-protein dependent pathway in the nervous system (26-28). α_2-Adrenoceptors couple to the inhibitory G_o/G_i-protein to inhibit adenylyl cyclase or to interact directly with calcium channels (28). Coupling between α_2-adrenoceptor and specific subtypes of voltage-gated calcium channels has not been studied myenteric neurons. This study was designed to identify the type of calcium channel that is inhibited following activation of the α_2-adrenoceptor in myenteric neurons and in their varicosities. These studies were done using whole-cell patch clamp techniques and calcium imaging methods to study Ca^{2+} dynamics in guinea-pig small intestinal myenteric neurons maintained in primary culture.

METHODS AND MATERIALS

All animal use protocols were approved by the Institutional Animal Use and Care Committee at Michigan State University.

Primary Culture of Myenteric Neurons

Newborn (1−2 days old) guinea pigs were killed by severing the major neck blood vessels after deep halothane anesthesia. The entire length of small intestine was placed in cold (4°C) sterile-filtered Krebs' solution of the following composition (millimolar): 120 NaCl, 5 KCl, 2.5 $CaCl_2$, 1.2 $MgCl_2$, 1.3 NaH_2PO_4, 25 $NaHCO_3$, and 11 glucose. The longitudinal muscle myenteric plexus was stripped free using a cotton swab and cut into 5-mm pieces. Tissues were divided into 4 aliquots, and each aliquot was transferred to 1 ml of Krebs' solution containing 1 mg/ml trypsin for 15−20 min at 37 °C. Tissues were then triturated 30 times and centrifuged at 900 *g* for 5 min using a bench-top centrifuge. The supernatant was discarded, and the pellet was resuspended and incubated (30 min, 37°C) in Krebs' solution containing 1 mg/ml collagenase. The suspension was triturated again 30 times and centrifuged at 900 *g* for 5 min. The pellet was suspended in minimum essential medium (MEM) containing 10% fetal bovine serum, gentamicin (10 μg/ml), penicillin (100 U/ml) and streptomycin (50 μg/ml). Cells were plated on glass cover slips coated with poly-L-lysine (50 μg/ml for 2 h) and maintained in an incubator at 37°C with 5% CO_2 for up to 2 weeks. After 2 days in culture, cytosine arabinoside (10 μM) was added to the MEM to limit smooth muscle and fibroblast proliferation. The medium was changed twice weekly.

Electrophysiological methods

Whole cell patch-clamp recordings were carried out at room temperature. Fire-polished patch pipettes with tip resistances of 3−6 MΩ were used for whole cell recordings. Seal resistances for all recordings were ≥ 5GΩ. The extracellular solution contained (millimolar): 97 NaCl, 20 tetraethylammonium, 4.7 CsCl, 5 $CaCl_2$, 1.2 $MgCl_2$, 1.2 NaH_2PO_4, 25 $NaHCO_3$, 11 glucose, and 0.0003 TTX. The pipette solution contained (millimolar): 160 CsCl, 2 $MgCl_2$, 10 EGTA, 10 HEPES, 1 ATP, and 0.25 GTP. The pH and osmolality for the extracellular solutions were adjusted to 7.2−7.4 (using CsOH or KOH) and 310−320 mosmol/kg H_2O (using CsCl). I_{Ca}^{2+} was recorded by depolarizing the membrane potential to −10 mV from a holding potential of −70 mV. All recordings were made using an Axopatch 200A amplifier (Axon Instruments,

Foster City, CA). Data were acquired using pClamp 6.0 (Axon Instruments) and currents were sampled at 5 kHz and were filtered at 2 kHz (4-pole Bessel filter).

Calcium imaging

The methods for measuring intracellular Ca^{2+} in myenteric neurons maintained in primary culture were similar to those published by others (29-32). Myenteric neurons grown on glass coverslips were loaded for 45 min at 37°C in Opti-MEM (Invitrogen, Carlsbad, CA) solution containing the calcium indicator dye, Fluo-4 AM (2 μM)(Molecular Probes, Inc., Eugene, OR) and Pluronic F-127 (1% v/v)(Molecular Probes). After Fluo-4 loading, cover slips containing neurons were transferred to a cover glass-based chamber mounted on a microscope (Olympus, IX 70). The chamber was perfused continuously with oxygenated (95 $\%O_2$, 5% CO_2) Krebs' solution. The Fluo-4 was excited at 488 nm using a high speed multi-wavelength illuminator (DeltaRam, Photon Technology, Inc., Birmingham, NJ) and fluorescence emission was collected in the 500 − 560 nm range using a CCD camera (8 bit acquisition, IC-100, Photon Technology) connected to the microscope. Ca^{2+} influx through voltage-gated calcium channels was evoked using elevated extracellular KCl (60 mM). $\Delta[Ca^{2+}]_i$ was calculated by subtracting the baseline fluorescence from the peak fluorescence measured during KCl depolarization; these values are expressed as arbitrary fluorescence units (AFU). Each cover slip of neurons was exposed to three successive applications of elevated KCl applied at 10 minute intervals. The first application was the control response while the second two applications occurred in the presence of drugs used to block the calcium response. Pilot studies revealed that the KCl-induced increases in calcium fluorescence declined significantly after 30 minutes. The acquired fluo-4 fluorescence signals were stored on a computer hard drive for subsequence analysis using ImageMaster software (Version 5.0, Photon Technology).

Drug application

In whole cell patch-clamp recordings, drugs were applied using an array of quartz, gravity-fed flow tubes (320 μm ID and 450 μm OD; Polymicron Technologies, Phoenix, AZ). The distance from the mouth of the tubes to the cell examined was about 200 μm, and the position of the tubes was controlled manually using a micromanipulator. For pertussis toxin treatment, myenteric neurons were incubated in MEM containing pertussis toxin (1 μM) for 2 hr before the patch-clamp experiments. For calcium imaging experiments, drugs were applied via addition to the bath perfusion solution.

Data Analysis

Effects of different treatments were compared using Student's t-test or repeated measures analysis of variance followed by Student Newman Keul's post hoc test. Data are expressed as mean ± s.e.m. and n values indicate the number of neurons from which data were obtained. $P < 0.05$ was considered statistically significant.

Drugs

ATP (Disodium salt, Sigma Chemical Co., St. Louis MO, A-3377); $CdCl_2$ (Sigma, C-3141); collagenase (EMD Biosciences, Inc. San Diego, CA) 234200); cytosine β-D-Arabinoside (Ara-C, Sigma, C-6645); fetal bovine serum (Sigma, F-2442); Fluo-4 AM (Molecular Probes, F-14201); Gentamicin (Sigma, G-1272); GTP (Sodium salt, Sigma, G-8752); minimum essential medium (MEM, Sigma, M-0268); $NiCl_2$ (Sigma, N-5756); nifedipine (Sigma, N-7634); Opti-MEM (GIBCO, 51985−034); penicillin/streptomycin (Sigma, P-0781); pertussis toxin (PTX, Sigma, P-7208); Pluronic F-127 (Molecular Probes, P-6866); poly-L-lysine (Sigma, P-2636); SNX 482 (Alomone, Inc. Jerusalem, Israel, S-500); tetraethylammonium chloride (TEA, Sigma, T-2265); tetrodotoxin (TTX, Sigma, T-5651);

trypsin (Sigma T-5266); UK 14,304 (Sigma, U-104); ω-Agatoxin IVA (ATX, Alomone, A-500); ω-Conotoxin GVIA (CTX, Alomone, C-300);

RESULTS

UK 14,304 inhibits I_{Ca2+}

UK 14,304 is a selective α2 adrenoceptor agonist (33) that has been used in a number of studies of α_2-adrenoceptors in the enteric nervous system (27,28). Therefore, we used this agonist to study the effects of α_2-adrenoceptor activation on I_{Ca}^{2+} in myenteric neurons. I_{Ca}^{2+} was activated by depolarizing the membrane potential from a holding potential of −70 mV to a test potential of −10 mV. I_{Ca}^{2+} did not decline during repeated depolarizations applied over 60 minutes as described previously (13). Direct measurements of soma I_{Ca}^{2+} using whole cell recording techniques showed that I_{Ca}^{2+} was inhibited by UK 14,304, in a concentration-dependent (0.0001 − 1 μM) and reversible manner (Fig. 1). At the maximum concentration (1 μM), UK 14,304 inhibited I_{Ca}^{2+} by 45.0 ± 6.4 % from −1.8 ± 0.3 nA to −1.0 ± 0.2 nA ($P < 0.05$, n = 7; Fig. 1).

UK 14,304 selectively inhibits R-type calcium channels

Myenteric neurons express functional N-, P/Q, L- and R-type Ca^{2+} channels (12,13). In the present study, it was found that the relative contribution of each Ca^{2+} channel subtype to the total current varied somewhat from cell-cell. In order to estimate the relative contributions of each channel type we determined the percent inhibition of the total Ca^{2+} current caused by ω-agatoxin (ATX, P/Q –type channel antagonist, 0.1 μM), (ω-conotoxin (CTX, N-type channel antagonist, 0.1 μM), nifedipine (L-type channel antagonist, 1 μM) and $NiCl_2$ (R-type channel antagonist, 50 μM) in 10 neurons. Based on these studies it was found that P/Q-type channels contributed 17 ± 2 % (range = 9 − 32%), L-type channels contributed 22 ± 2% (range = 15 − 40%), N-type channels contributed 29 ± 4% (range = 13 − 48%) and R-type channels contributed 45 ± 3% (range = 29 − 57%).

We next investigate the actions of UK 14,304 on I_{Ca}^{2+} carried by specific Ca^{2+} channel subtypes. In these neurons, nifedipine (1 μM) reduced I_{Ca}^{2+} by 19 ± 1% from −1.6 ± 0.2 to −1.3 ± 0.2 nA ($P < 0.05$, n = 5; Fig. 2A,B). UK 14,304 (1 μM) inhibited nifedipine-resistant I_{Ca}^{2+} by 54 ± 2.0 % to −0.7 ± 0.09 nA ($P < 0.001$, n = 5). I_{Ca}^{2+} recovered after washing with nifedipine-containing solution (n = 4; Fig. 2B).

ATX (0.1 μM), reduced I_{Ca}^{2+} by 20 ± 4% from −0.9 ± 0.1 to −0.7 ± 0.06 nA ($P < 0.01$, n = 5; Fig. 3). In the presence of ATX, UK 14,304 (1 μM) reversibly inhibited I_{Ca}^{2+} by 50 ± 3% to 0.4 ± 0.05 nA ($P < 0.001$, n = 5; Fig. 3A,B).

CTX (0.1 μM), reduced I_{Ca}^{2+} by ~35%. In the presence of CTX, UK 14.304 (1 μM) reversibly reduced I_{Ca}^{2+} by 22 ± 3 % from −0.96 ± 0.1 to −0.7 ± 0.1 nA ($P < 0.05$, n = 8; Fig. 4A,B).

$NiCl_2$ (50 μM), inhibited I_{Ca}^{2+} by 47 ± 3% from −1.6 ± 0.2 to −0.9 ± 0.1 nA ($P < 0.05$, n = 6; Fig. 5A,B). In the presence of $NiCl_2$ (50 μM), UK 14,304 (1 μM) did not further reduce I_{Ca}^{2+} ($P > 0.05$, n = 6; Fig. 5B). The effect of UK 14,304 on I_{Ca}^{2+} in the presence of the specific R-type Ca^{2+} channel toxin, SNX-482 (0.1 μM), was also tested. In these experiments the mean control I_{Ca}^{2+} was −1.1 ± 0.2 nA (n = 5) and SNX-482 reduced I_{Ca}^{2+} by 44 ± 4% to −0.6 ± 0.1 nA ($P < 0.05$, n = 5; Fig. 5C,D). Subsequent application of UK 14,304 did not further reduce I_{Ca}^{2+} ($P > 0.05$, n = 5; Fig. 5C,D). I_{Ca}^{2+} recovered after washing with drug-free Krebs' solution (Fig. 5D).

Inhibitory effect of UK 14,304 on I_{Ca}^{2+} is blocked by pertussis toxin

After pertussis toxin treatment, activation of α_2-adrenoceptor by UK 14,304 (1 μM) failed to alter I_{Ca}^{2+} significantly ($P > 0.05$, n = 5, Fig. 6A,B).

UK 14,304 inhibits R-type Ca^{2+} channels in the soma and varicosities

$\Delta[Ca^{2+}]_i$ in the soma and varicosities was evoked by depolarizing the membrane potential with KCl (60 mM). Varicosites were identified visually as periodic swellings in nerve fibers (Fig. 7A). Many of these varicosities were in close proximity to individual soma suggesting that these might be the sites of synaptic contact (Fig. 7B). We verified that $\Delta[Ca^{2+}]_I$ in varicosities did not require axonal conduction by testing the effects of the sodium channel blocker, tetrodotoxin (TTX, 0.3 μM) on $\Delta[Ca^{2+}]_i$. These data show that TTX reduced the calcium signal by about 20% indicating that sodium channel dependent action potentials contributed to the calcium signal. However, the $\Delta[Ca^{2+}]_I$ is due predominately to action potential independent activation of voltage-gated Ca^{2+} channels (Fig. 7C,D).

In the next set of experiments, we verified the stability of the KCl-induced $\Delta[Ca^{2+}]_i$ over the time course of our studies. It was found that $\Delta[Ca^{2+}]_i$ did not decline significantly in either nerve cell bodies or in varicosities during 3 successive KCl applications over a 20 minute period, the time course of subsequent experiments (Fig. 8A,B).

$\Delta[Ca^{2+}]_i$ was measured in the soma and in varicosities of individual myenteric neurons (Fig. 9A,B). While drug-induced effects on I_{Ca}^{2+} can be measured directly in the soma it is more difficult to measure drug-induced changes in I_{Ca}^{2+} varicosities. We used $\Delta[Ca^{2+}]_i$ as an indirect measure of I_{Ca}^{2+} in varicosities. UK 14,304 (1 μM) inhibited $\Delta[Ca^{2+}]_i$ in the cell soma by 48 ± 8% (from 56 ± 11 to 30 ± 7 AFU; $P < 0.05$, n = 6; Fig. 9B). UK 14,304 (1 μM) also inhibited $\Delta[Ca^{2+}]_i$ in varicosities by 44 ± 5% (from 10 ± 2 to 6 ± 2 AFU; $P < 0.05$, n = 7; Fig. 9B). The $\Delta[Ca^{2+}]_i$ evoked by KCl (60 mM) was abolished by $CdCl_2$ (100 μM) in both the cell soma and in varicosities (Fig. 9A,B).

$NiCl_2$ (50 μM) inhibited soma $\Delta[Ca^{2+}]_i$ evoked by KCl depolarization by 55 ± 5% from 45 ± 6 to 20 ± AFU ($P < 0.05$, n = 4; Fig. 10A,B). In the presence of $NiCl_2$ (50 μM), UK 14,304 (1 μM) did not alter $\Delta[Ca^{2+}]_i$ ($P > 0.05$, n = 4; Fig. 10A,B). In 4 of 5 varicosities, $NiCl_2$ (50 μM) inhibited $\Delta[Ca^{2+}]_i$ by 47 ± 7% from 5.2 ± 0.8 AFU to 2.6 ± 0.3 AFU ($P < 0.05$, n = 4; Fig. 10A,B). In the presence of $NiCl_2$ (50 μM) further application of UK 14,304 (1 μM) also did not alter $\Delta[Ca^{2+}]_i$ ($P > 0.05$, n = 4; Fig. 10A,B). Similarly, SNX- 482 (0.1 μM) inhibited $\Delta[Ca^{2+}]_i$ in the cell soma and in varicosities and UK 14,304 failed to inhibit $\Delta[Ca^{2+}]_i$ in the presence of the R-type Ca^{2+} channel blocker (Fig. 11).

DISCUSSION

Previous work showed that, in guinea pig small intestinal myenteric neurons, total I_{Ca}^{2+} is composed of currents contributed by L- N- P/Q- and R-type voltage-gated calcium channels (12,13). In the present study, we found that I_{Ca}^{2+} was inhibited in a concentration-dependent manner by the selective α_2-adrenoceptor agonist, UK 14,304. UK 14,304-induced inhibition of I_{Ca}^{2+} persisted after L- N- and P/Q-type channels were blocked indicating that the α_2-adrenoceptor does not couple to inhibition of those Ca^{2+} channel subtypes. However, when the R-type Ca^{2+} channel was blocked by low concentrations of $NiCl_2$ or by SNX-482, UK 14,304 no longer inhibited I_{Ca}^{2+}. Previous work showed that α2-adrenoceptors couple to inhibition of Ca^{2+} channels in guinea pig small intestinal submucosal neurons where α_2-adrenoceptors couple specifically to inhibition of N-type Ca^{2+} channels (36). However, our data demonstrate that α_2-adrenoceptors selectively couple to inhibition of R-type calcium channels in guinea pig small intestinal myenteric neurons. The differential coupling of α_2-

adrenoceptors to N- and R-type Ca^{2+} channels may be related to differential expression of Ca^{2+} channel subtypes in the two enteric plexuses. Immunohistochemical studies have shown that the subunits forming N-type channels (α1B) are expressed by myenteric and submucosal neurons (36) while α_{1E} subunits (forming R-type Ca^{2+} channels) are expressed only in the myenteric plexus (37). Therefore, R-type Ca^{2+} channels would be available for modulation by α_2-adrenoceptors only in the myenteric plexus.

It is possible that our recording conditions favored R-type calcium channel modulation by α2 adrenoceptors as the high extracellular Ca^{2+} concentration (5 mM) could favor the function of one channel subtype over another. The single channel conductance of the calcium channel subtypes (10−20 pS) expressed by myenteric neurons are similar, so elevated Ca^{2+} does not favor one channel over another in terms of peak current. However, there are differences in Ca^{2+}-dependent mechanisms controlling channel activation and inactivation (19). L-type Ca^{2+}channels in muscle exhibit a rapid calcium dependent inactivation while N and P/Q type channels exhibit both Ca^{2+}-dependent inhibition and excitation under different activation conditions. The protocol we used in which Ca^{2+} currents were activated by single voltage commands applied at 10 s intervals would minimize the contribution of these Ca^{2+} dependent mechanisms modulating channel activity.

R-type Ca^{2+} channels are localized to cell bodies of neurons throughout the nervous system (23,36-38) and these Ca^{2+} channels have several functions. For example, R-type Ca^{2+} channels regulate action potential firing in hippocampal CA1 pyramidal neurons (39). While R-type Ca^{2+} channels are responsible for 50% of the total voltage-gated $I_{Ca}{}^{2+}$ in myenteric neurons (13), their function has not yet been established. R-type calcium channels in myenteric neurons require strong depolarizations and currents carried by R-channels have fast activation kinetics (3). These attributes would allow them to contribute to Ca^{2+} entry during action potentials in the somatodendritic region of myenteric neurons. Ca^{2+} entry through R-type channels may play a role in action potential firing patterns in the myenteric plexus. α_2-adrenoceptors are localized to the soma of guinea pig ileum myenteric neurons (34,40). These receptors are targets for norepinephrine released by sympathetic nerves supplying the small intestine and activation of sympathetic nerves inhibits enteric neurons (25,34,35). α_2-adrenoceptor-mediated inhibition of R-type Ca^{2+} currents could modulate action potential duration or firing rate in myenteric neurons.

α_2-Adrenoceptors couple to the inhibitory G_O/G_I G-proteins (28,35,36,41,42). In the present study, the inhibitory effect of UK 14,304 on $I_{Ca}{}^{2+}$ was blocked by pertussis toxin, a selective G_O/G_I G-protein toxin. This result confirms previous studies done in submucosal neurons showing that α_2-adrenoceptors couple to inhibition of voltage-gated Ca^{2+} channels via pertussis toxin sensitive G-protein (36). However, we have shown for the first time that R-type Ca^{2+} channels are a specific target for α_2-adrenoceptor-mediated inhibition. The signaling cascade that links the α_2-adrenoceptor to the R-type Ca^{2+} channel inhibition in guinea-pig myenteric neurons has yet to be elucidated. However, it has been established that in submucosal neurons α_2-adrenoceptors activate a membrane-delimited, G-protein-dependent pathway where G_O interacts directly with Ca^{2+} channels to decrease their open probability (43). It is likely that R-type Ca^{2+} channels in myenteric neurons are inhibited by α_2-adrenoceptors via a similar mechanism. In addition to coupling to inhibition of Ca^{2+} channels, α_2-adrenoceptors can also couple via a G_o-dependent mechanism to activation of K^+ channels and membrane hyperpolarization (36). α_2-adrenoceptor mediated hyperpolarizations are very prominent in submucous plexus neurons and the hyperpolarization accounts for a large part of the inhibitory effect of norepinephrine on these cells (36). However, α_2-adrenoceptor-mediated hyperpolarization is detected only occasionally in studies using intracellular electrodes to record from neurons in the acutely isolated myenteric plexus preparation (34). Therefore, the

most prominent effect of α_2-adrenoceptors activation in the myenteric plexus is likely to be direct inhibition of Ca^{2+} channels via the G_o/G_i-dependent mechanism.

We did not establish the electrophysiological classification of the neurons from which recordings were obtained because TTX and K^+ channel blockers (TEA and Cs^+) were present in the recording solutions throughout these studies. TTX will block synaptic transmission; therefore, we were unable to record the fast excitatory postsynaptic potentials that are a property of S neurons (3). The K^+ channel blockers we used would block the slow action potential afterhyperpolarization that is characteristic of AH-type neurons (3). Our previous study (9) showed that R-type Ca^{2+} currents were recorded from 90% of myenteric neurons maintained in primary culture. However, in the absence of data obtained from phenotypically-identified neurons, it is not possible for us to conclude that R-type Ca^{2+} channels are expressed by both S and AH type neurons. Similarly, we showed that the inhibitory affect of α_2-adrenoceptor activation on R-type Ca^{2+} currents was observed in almost all neurons but in the absence of phenotypic identification we can not conclude that this effect occurs in both S and AH type neurons.

The data described above indicate that α_2-adrenoceptors couple selectively to inhibition of R-type Ca^{2+} channels located to nerve cell bodies. However, the principal site of action for norepinephrine in the myenteric plexus is on nerve endings where norepinephrine acts to inhibit neurotransmitter release (25,34). Detailed characterization of Ca^{2+}-dependent mechanisms in myenteric neuronal varicosities is difficult because their small size makes them inaccessible to studies using micro- or patch clamp electrodes. However, imaging techniques using Ca^{2+}-sensitive fluorescent probes, such as Fluo-4, and photometry provide an opportunity to study Ca^{2+} in individual varicosities. In these Ca^{2+} imaging studies, activation of voltage-gated Ca^{2+} channels was accomplished by raising extracellular KCl from 5 to 60 mM. This would change the membrane potential of neurons and varicosities to approximately −20 mV, a level similar to that used to activate Ca^{2+} channels in the patch clamp studies. KCl-induced depolarization evoked a $CdCl_2$-sensitive increase in Fluo-4 fluorescence in the soma and varicosities of myenteric neurons indicating that this signal was due to Ca^{2+} influx through voltage-gated calcium Ca^{2+}. This provided an opportunity to study the contribution of R-type Ca^{2+}channels to Ca^{2+} entry into varicosities and to study α_2-adrenoceptor modulation of these channels.

$NiCl_2$, at a concentration that is selective for R-type Ca^{2+} channels, and SNX-482 reduced the Ca^{2+} signal in the soma and nerve terminals by about 50%. Our whole-cell patch clamp data showed that the R-type Ca^{2+} channel carried up to 50% of the total $I_{Ca}{}^{2+}$. Therefore, half of the KCl-evoked calcium signal measured in the cell soma and in varicosities is due to activation of R-type Ca^{2+} channels. The KCl-evoked Ca^{2+} signals in the cell soma and in varicosities were reduced by approximately 50% by UK 14,304. In addition, when the Ca^{2+} signal was reduced by $NiCl_2$ or SNX-482, UK 14,304 did not produce a further inhibition of this response. These data are similar to the UK 14,304-induced inhibition of $I_{Ca}{}^{2+}$ measured in the cell soma using whole-cell recording. Based on these data we conclude that α_2-adrenoceptors expressed by myenteric neuronal varicosities couple selectively to inhibition of R-type Ca^{2+} channels.

α_2-adrenoceptors mediate presynaptic inhibition of fast and slow excitatory synaptic transmission in the ENS (34,44,45). The α_2-adrenoceptors are the target for sympathetic nervous system modulation of synaptic transmission and R-type Ca^{2+} channels may be one target for nerve-released norepinephrine. However, previous studies have shown that N, and P/Q type Ca^{2+} channels make major contributions to the calcium entry into nerve terminals required for neurotransmitter release from myenteric neurons (14-18). The contribution of R-type Ca^{2+} channels to the release of fast or slow excitatory synaptic transmitters in the myenteric plexus remains to be determined.

CONCLUSION

In guinea-pig small intestinal myenteric neurons, activation of the α_2-adrenoceptor selectively inhibits the R-type Ca^{2+} channels via a G_i/G_o-protein-linked pathway. As sympathetic nerve fibers contact the soma-dendritic region and varicosities in the myenteric plexus (46,47), α_2-adrenoceptor-mediated inhibition of R-type Ca^{2+} channels may be a mechanism by which norepinephrine can regulate myenteric neuron excitability and/or neurotransmitter release.

ACKNOWLEDGEMENT

This work was supported by National Institutes of Health Grant DK57039.

REFERENCES

1. Furness, JB. The enteric nervous system. Vol. 1st edition. Blackwell Publishing, Incorporated; 2006.
2. Kunze WA, Furness JB. The enteric nervous system and regulation of intestinal motility. Ann Rev Physiol 1999;61:117–42. [PubMed: 10099684]
3. Hirst GDS, Holman ME, Spence I. Two types of neurones in the myenteric plexus of duodenum in the guinea-pig. J Physiol 1974;236:303–26. [PubMed: 16992436]
4. Furness JB, Jones C, Nurgali K, Clerc N. Intrinsic primary afferent neurons and nerve circuits within the intestine. Prog Neurobiol 2004;72:143–64. [PubMed: 15063530]
5. Vogalis F, Furness JB, Kunze WA. Afterhyperpolarization current in myenteric neurons of the guinea pig duodenum. J Neurophysiol 2001;85:1941–51. [PubMed: 11353011]
6. Hillsley K, Kenyon JL, Smith TK. Ryanodine-sensitive stores regulate the excitability of AH neurons in the myenteric plexus of guinea-pig ileum. J Neurophysiol 2000;84:2777–85. [PubMed: 11110808]
7. Vanden Berghe P, Kenyon JL, Smith TK. Mitochondrial Ca2+ uptake regulates the excitability of myenteric neurons. J Neurosci 2002;22:6962–71. [PubMed: 12177194]
8. North RA. The calcium-dependent slow after-hyperpolarization in myenteric plexus neurones with tetrodotoxin-resistant action potentials. Br J Pharmacol 1973;49:709–11. [PubMed: 4788043]
9. Hirst GD, Johnson SM, van Helden DF. The slow calcium-dependent potassium current in a myenteric neurone of the guinea-pig ileum. J Physiol 1985;361:315–37. [PubMed: 2580979]
10. Brookes SJ. Classes of enteric nerve cells in the guinea-pig small intestine. Anat Rec 2001;262:58–70. [PubMed: 11146429]
11. Shuttleworth CW, Smith TK. Action potential-dependent calcium transients in myenteric S neurons of the guinea-pig ileum. Neuroscience 1999;92:751–62. [PubMed: 10408623]
12. Smith TK, Kang SH, Vanden Berghe P. Calcium channels in enteric neurons. Curr Opin Pharmacol 2003;3:588–93. [PubMed: 14644009]
13. Bian X, Zhou X, Galligan JJ. R-type calcium channels in myenteric neurons of guinea pig small intestine. Am J Physiol 2004;287:G134–42.
14. Reis HJ, Massensini AR, Prado MA, Gomez RS, Gomez MV, Romano-Silva MA. Calcium channels coupled to depolarization-evoked glutamate release in the myenteric plexus of guinea-pig ileum. Neuroscience 2000;101:237–42. [PubMed: 11068152]
15. Garaulet JV, Laorden ML, Milanes MV. Effect of chronic administration of dihydropyridine Ca^{2+} channel ligands on sufentanil-induced tolerance to mu- and kappa-opioid agonists in the guinea pig ileum myenteric plexus. Reg Pep 1996;63:1–8.
16. Starodub AM, Wood JD. Selectivity of omega-CgTx-MVIIC toxin from Conus magus on calcium currents in enteric neurons. Life Sci 1999;64:PL305–10. [PubMed: 10403514]
17. Takahashi T, Tsunoda Y, Lu Y, Wiley J, Owyang C. Nicotinic receptor-evoked release of acetylcholine and somatostatin in the myenteric plexus is coupled to calcium influx via N-type calcium channels. J Pharmacol Exp Ther 1992;263:1–5. [PubMed: 1357155]
18. Tran S, Boot JR. Differential effects of voltage-dependent Ca2+ channels on low and high frequency mediated neurotransmission in guinea-pig ileum and rat vas deferens. Eur J Pharmacol 1997;335:31–6. [PubMed: 9371543]

19. Catterall WA. Structure and regulation of voltage-gated Ca2+ channels. Ann Rev Cell Develop Biol 2000;16:521–55.
20. Sochivko D, Pereverzev A, Smyth N, Gissel C, Schneider T, Beck H. The Ca(V)2.3 Ca(2+) channel subunit contributes to R-type Ca(2+) currents in murine hippocampal and neocortical neurones. J Physiol 2002;542:699–710. [PubMed: 12154172]
21. Newcomb R, Szoke B, Palma A, Wang G, Chen X, Hopkins W, Cong R, Miller J, Urge L, Tarczy-Hornoch K, Loo JA, Dooley DJ, Nadasdi L, Tsien RW, Lemos J, Miljanich G. Selective peptide antagonist of the class E calcium channel from the venom of the tarantula Hysterocrates gigas. Biochemistry 1998;37:15353–62. [PubMed: 9799496]
22. Randall A, Tsien RW. Pharmacological dissection of multiple types of Ca2+ channel currents in rat cerebellar granule neurons. J Neurosci 1995;15:2995–3012. [PubMed: 7722641]
23. Tottene A, Volsen S, Pietrobon D. alpha(1E) Subunits form the pore of three cerebellar R-type calcium channels with different pharmacological and permeation properties. J Neurosci 2000;20:171–8. [PubMed: 10627594]
24. Paton WD, Vizi ES. The inhibitory action of noradrenaline and adrenaline on acetylcholine output by guinea-pig ileum longitudinal muscle strip. Br J Pharmacol 1969;35:10–28. [PubMed: 4302725]
25. Stebbing M, Johnson P, Vremec M, Bornstein J. Role of alpha(2)-adrenoceptors in the sympathetic inhibition of motility reflexes of guinea-pig ileum. J Physiol 2001;534:465–78. [PubMed: 11454964]
26. Boehm S, Huck S. alpha 2-Adrenoreceptor-mediated inhibition of acetylcholine-induced noradrenaline release from rat sympathetic neurons: an action at voltage-gated Ca2+ channels. Neuroscience 1995;69:221–31. [PubMed: 8637620]
27. Xu ZJ, Adams DJ. Alpha-adrenergic modulation of ionic currents in cultured parasympathetic neurons from rat intracardiac ganglia. J Neurophysiol 1993;69:1060–70. [PubMed: 8098358]
28. Dolphin AC. Mechanisms of modulation of voltage-dependent calcium channels by G proteins 1998;506:3–11.
29. Kimball BC, Yule DI, Mulholland MW. Caffeine- and ryanodine-sensitive Ca^{2+} stores in cultured guinea pig myenteric neurons. Am J Physiol 1996;270:G594–603. [PubMed: 8928789]
30. Christofi FL, Guan Z, Wood JD, Baidan LV, Stokes BT. Purinergic Ca^{2+} signaling in myenteric neurons via P_2 purinoceptors. Am J Physiol 1997;272:G463–73. [PubMed: 9124566]
31. Vanden Berghe P, Tack J, Coulie B, Andrioli A, Bellon E, Janssens J. Synaptic transmission induces transient Ca^{2+} concentration changes in cultured myenteric neurones. Neurogastroenterol Motil 2000;12:117–24. [PubMed: 10771494]
32. Vogalis F, Hillsley K, Smith T. Recording ionic events from cultured, Dil-labelled myenteric neurons in the guinea-pig proximal colon. J Neurosci Methods 2000;96:25–34. [PubMed: 10704668]
33. Cambridge D. UK 14,304, a potent and selective α2 agonist for the characterisation of α-adrenoceptor subtypes. Eur J Pharmacol 1981;72:413–15. [PubMed: 6115759]
34. Galligan JJ, North RA. Opioid, 5-HT_{1A} and $alpha_2$ receptors localized to subsets of guinea-pig myenteric neurons. J Auton Nerv Syst 1991;32:1–11. [PubMed: 1673695]
35. Surprenant A, North RA. Mechanism of synaptic inhibition by noradrenaline acting at alpha2-adrenoceptors. Proc R Soc Lond B Biol Sci 1988;234:85–114. [PubMed: 2901110]
36. Surprenant A, Shen KZ, North RA, Tatsumi H. Inhibition of calcium currents by noradrenaline, somatostatin and opioids in guinea-pig submucosal neurones. J Physiol 1990;431:585–608. [PubMed: 1983121]
37. Naidoo V, Bian X, Galligan JJ. Distribution of R-type calcium channels in the enteric nervous system of the guinea pig. Gastroenterology 2006;130(Suppl 2):A382.
38. Kirchgessner AL, Liu MT. Differential localization of Ca^{2+} channel alpha1 subunits in the enteric nervous system: presence of alpha1B channel-like immunoreactivity in intrinsic primary afferent neurons. J Comp Neurol 1999;409:85–104. [PubMed: 10363713]
39. Foehring RC, Mermelstein PG, Song WJ, Ulrich S, Surmeier DJ. Unique properties of R-type calcium currents in neocortical and neostriatal neurons. J Neurophysiol 2000;84:2225–36. [PubMed: 11067968]
40. Nasser Y, Ho W, Sharkey KA. Distribution of adrenergic receptors in the enteric nervous system of the guinea pig, mouse, and rat. J Comp Neurol 2006;495:529–53. [PubMed: 16498685]10

41. Hill CE, Powis DA, Hendry IA. Involvement of pertussis toxin-sensitive and - insensitive mechanisms in alpha-adrenoceptor modulation of noradrenaline release from rat sympathetic neurones in tissue culture. Br J Pharmacol 1993;110:281–8. [PubMed: 8106104]

42. Boehm S, Huck S, Drobny H, Singer EA. Pertussis toxin abolishes the inhibition of Ca2+ currents and of noradrenaline release via alpha$_2$-adrenoceptors in chick sympathetic neurons. Naunyn Schmiedebergs Arch Pharmacol 1992;345:606–9. [PubMed: 1356237]

43. Shen KZ, Surprenant A. Noradrenaline, somatostatin and opioids inhibit activity of single HVA/N-type calcium channels in excised neuronal membranes. Pflugers Arch 1991;418:614–6. [PubMed: 1682876]

44. Schemann M. Excitatory and inhibitory effects of norepinephrine on myenteric neurons of the guinea-pig gastric corpus. Pflugers Arch 1991;418:575–80. [PubMed: 1658726]

45. Dobreva G, Neunlist M, Frieling T, Schemann M. Post- and presynaptic effects of norepinephrine in guinea-pig colonic submucous plexus. Neurogastroenterol Motil 1998;10:123–30. [PubMed: 9614670]

46. Manber L, Gershon MD. A reciprocal adrenergic-cholinergic axoaxonic synapse in the mammalian gut. Am J Physiol 1979;236:E738–45. [PubMed: 443427]

47. Llewellyn-Smith IJ, Wilson AJ, Furness JB, Costa M, Rush RA. Ultrastructural identification of noradrenergic axons and their distribution within the enteric plexuses of the guinea-pig small intestine. J Neurocytol 1981;10:331–52. [PubMed: 7031192]

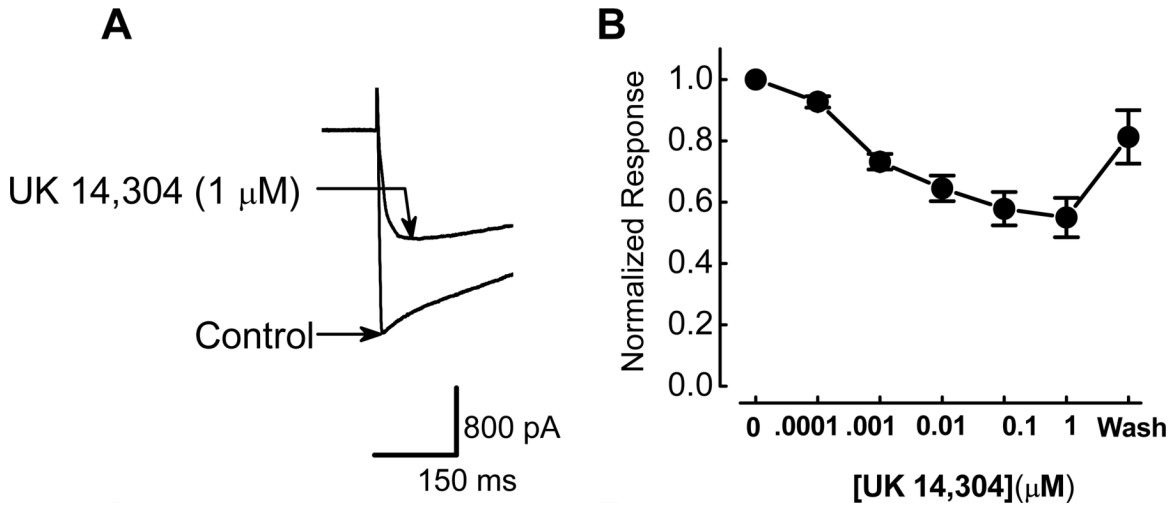

Figure 1.

Inhibitory effect of UK 14,304 on I_{Ca}^{2+}. A, Activation of α_2-adrenoceptors with UK 14,304 inhibited I_{Ca}^{2+}. I_{Ca}^{2+} was activated by depolarizing the membrane potential from −70 mV to −10 mV. B, Concentration-response relationship for UK 14,304 induced inhibition of I_{Ca}^{2+}. Inhibition of I_{Ca}^{2+} is plotted as amplitude in the presence of each concentration of UK 14,304 normalized to the control I_{Ca}^{2+}. Points represent the mean ± s.e.m. of data from 4−7 cells.

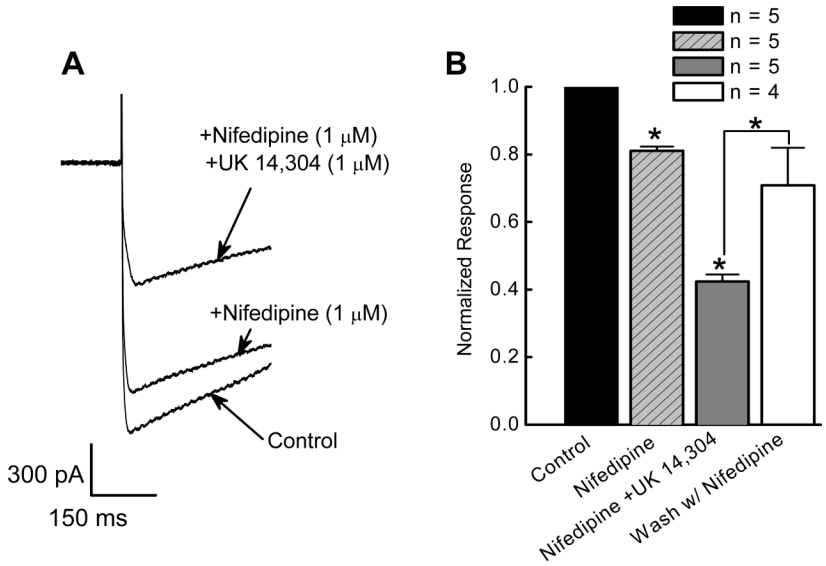

Figure 2.

Inhibitory effect of UK 14,304 on I_{Ca}^{2+} in the presence of the L-type channel antagonist, nifedipine. A, Representative recordings of I_{Ca}^{2+} showing a reduction by nifedipine and a further inhibition by addition of UK 14,304. B, Effect of UK14,304 (1 μM) to I_{Ca}^{2+} in the presence of nifedipine (1 μM). Currents recorded in the presence of nifedipine and UK 14,304 were normalized to the control current in the same neuron. The inhibitory effects of UK 14,304 were reversible on washing with nifedipine-containing Krebs' solution (n = 4). I_{Ca}^{2+} was activated by depolarizing the membrane potential from −70 mV to −10 mV.

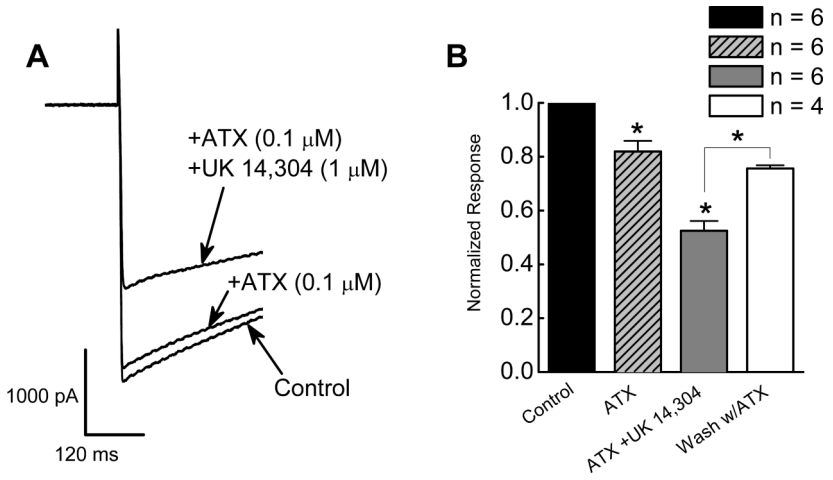

Figure 3.

Inhibitory effect of UK 14,304 on I_{Ca}^{2+} in the presence of ω-agatoxin IVA (ATX), a P/Q-type channel toxin. A, UK 14,304 inhibited I_{Ca}^{2+} in the presence ATX. I_{Ca}^{2+} was activated by depolarizing the membrane potential from −70 mV to −10 mV. B, UK14,304 inhibits I_{Ca}^{2+} in the presence of ATX. Currents recorded in the presence of ATX and UK 14,304 were normalized to the control current in the same neuron. ATX alone reduced I_{Ca}^{2+} significantly ($P < 0.05$). In the presence of ATX, UK 14,304 (1 μM) further inhibited I_{Ca}^{2+} ($P < 0.05$). The inhibitory effect of UK 14,304 was reversible by washing with ATX-containing Krebs' solution (n = 4).

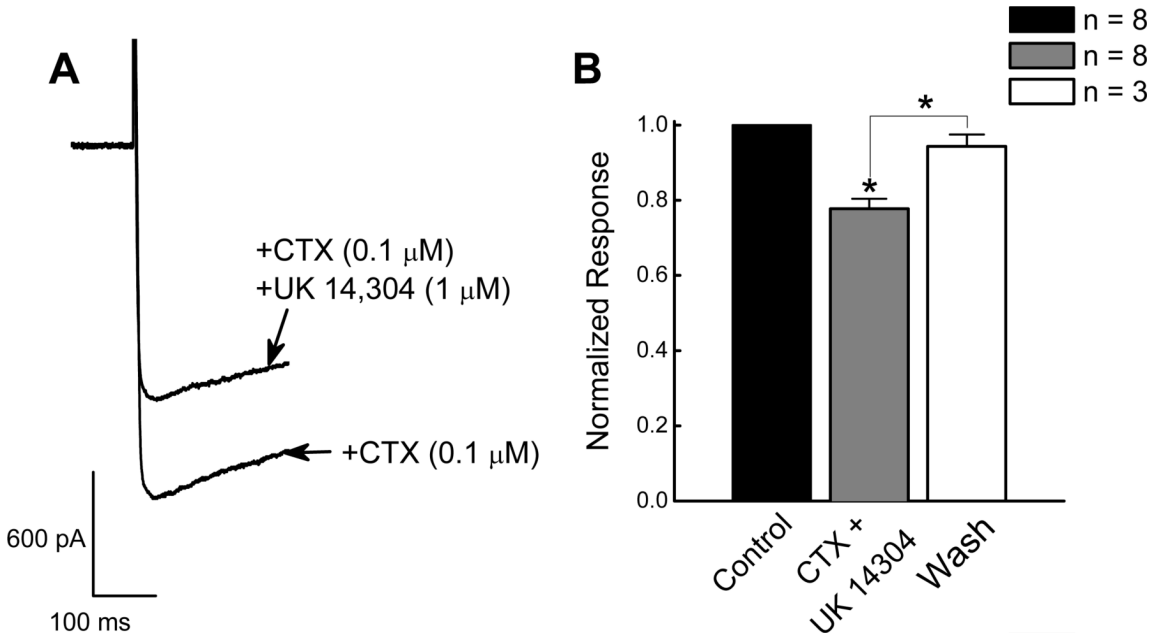

Figure 4.

Inhibitory effect of UK 14,304 on I_{Ca}^{2+} in the presence of an N-type Ca^{2+} channel toxin. A, UK 14,304 inhibited I_{Ca}^{2+} in the presence of CTX. I_{Ca}^{2+} was activated by depolarizing the membrane potential from −70 mV to −10 mV. B, Inhibitory effect of UK 14,304 on I_{Ca}^{2+} in the presence of CTX. CTX inhibited I_{Ca}^{2+} ($P < 0.05$) and UK 14.304 (1 μM) produced a further reduction in current amplitude ($P < 0.05$, $n = 8$). Currents recorded in the presence of CTX with 14,304 were normalized to the current recorded in the presence of CTX in the same neuron.

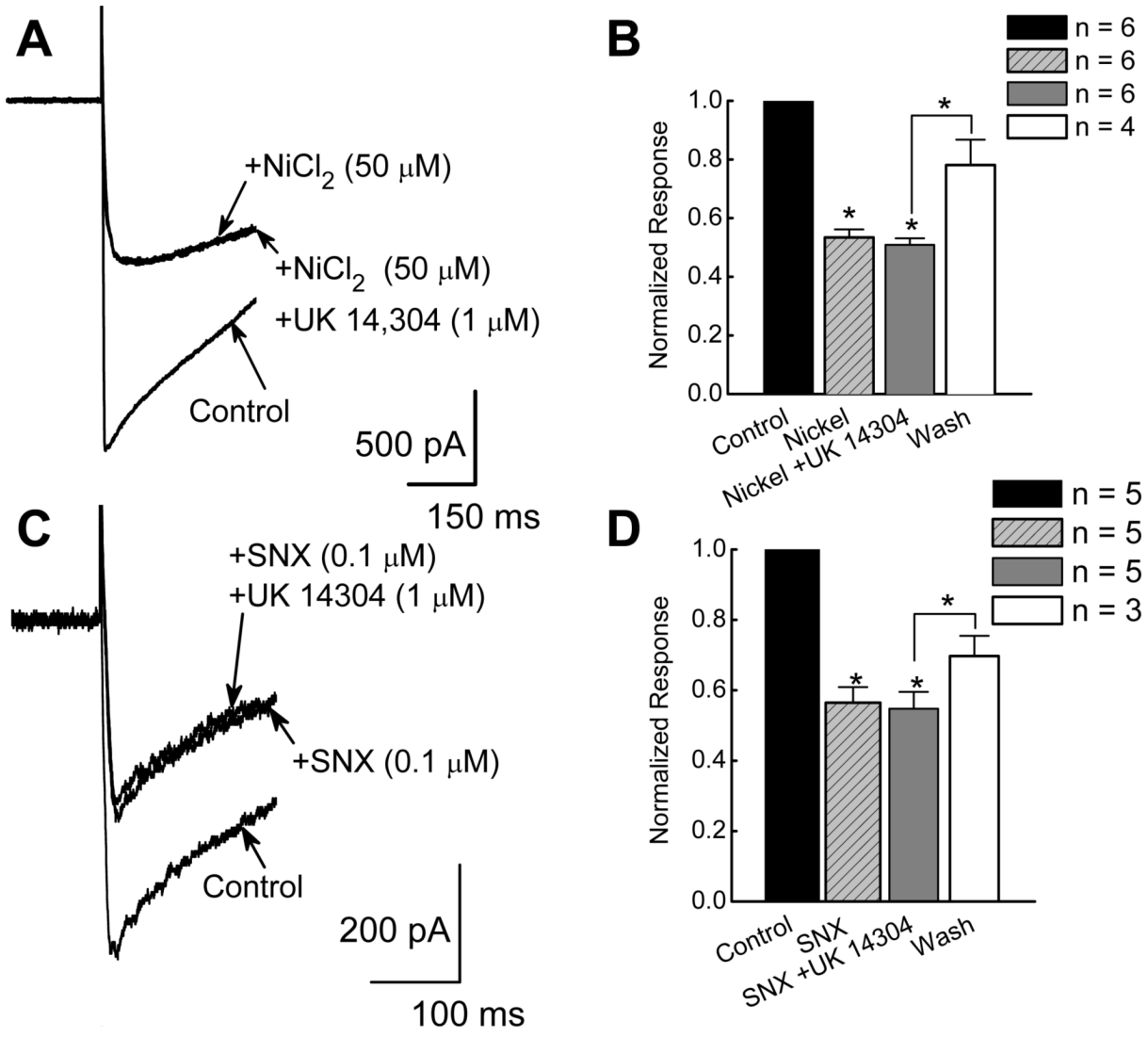

Figure 5.

UK 14,304 does not inhibit I_{Ca}^{2+} in the presence of R-type Ca^{2+} channel blockers. A and C, Original recordings of I_{Ca}^{2+} show that UK 14,304 did not alter I_{Ca}^{2+} in the presence $NiCl_2$ (A) or SNX-482 (C). B and D, Lack of effect of UK14,304 on I_{Ca}^{2+} in the presence of R-type Ca^{2+} channel toxins. I_{Ca}^{2+} was inhibited by $NiCl_2$ (B, $P < 0.05$, $n = 6$) and SNX-482 (D, $P < 0.05$, $n = 5$). In the presence of $NiCl_2$ or SNX-482 (D, $n = 5$), UK 14,304 did not further reduce I_{Ca}^{2+} ($P > 0.05$). In both cases, washing with blocker free Krebs' solution restored I_{Ca}^{2+} ($n = 3$ for $NiCl_2$ in B, $n = 4$ for SNX 482 in D). I_{Ca}^{2+} in the presence of blockers was normalized to the current amplitude recorded under control conditions.

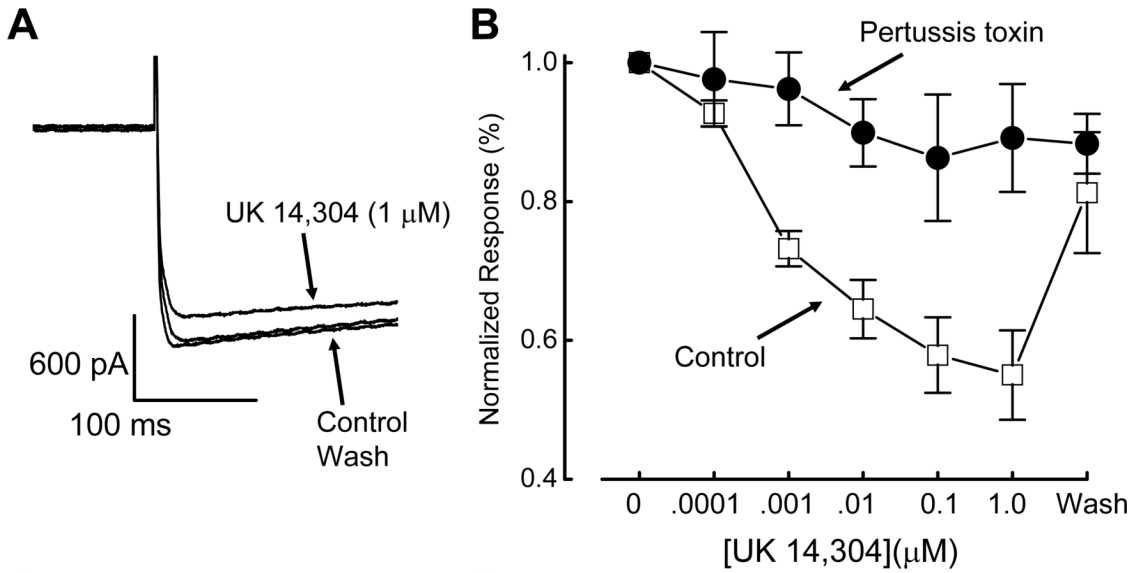

Figure 6.

PTX blocks the inhibitory effect of UK 14,304 on I_{Ca}^{2+}. A, The inhibitory effect of UK 14,304 (1 μM) on I_{Ca}^{2+} was blocked by PTX. I_{Ca}^{2+} activated by depolarizing the membrane potential to − 10 mV from a holding potential of −70 mV. B, PTX pretreatment blocks UK 14,304-induced inhibition of I_{Ca}^{2+}. I_{Ca}^{2+} was plotted as the mean current normalized to current amplitude before UK 14,304 application. Data are mean ± s.e.m. (n = 5).

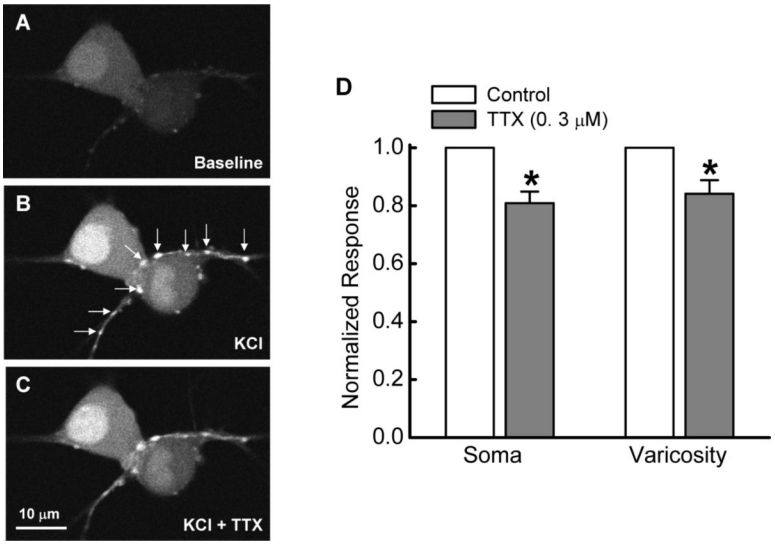

Figure 7.

$\Delta[Ca^{2+}]_i$ caused be elevated KCl (60 mM) in cell soma and in varicose nerve fibers. A-C, Images of Fluo-4 fluorescence in two neurons and in a varicose nerve fiber. A shows baseline fluorescence, B shows $\Delta[Ca^{2+}]_i$ in the presence of KCl (60 mM) and C shows the $\Delta[Ca^{2+}]_i$ response in the presence of tetrodotoxin (0.3 μM, TTX). Arrows in "B" show the position of varicosities. D, Mean data from 3 experiments similar to that shown in A-C. Data were obtained from 6 neurons and 14 varicosities. TTX significantly reduced $\Delta[Ca^{2+}]_i$ but did not block this response ($P < 0.05$, Student's t-test for paired data). These data indicate axonal conduction contributed to the $\Delta[Ca^{2+}]_i$ response axonal conduction was not an absolute requirement. The $\Delta[Ca^{2+}]_i$ response was due largely to depolarization-induced activation of voltage-gated Ca^{2+} channels in the cell soma and in varicosities.

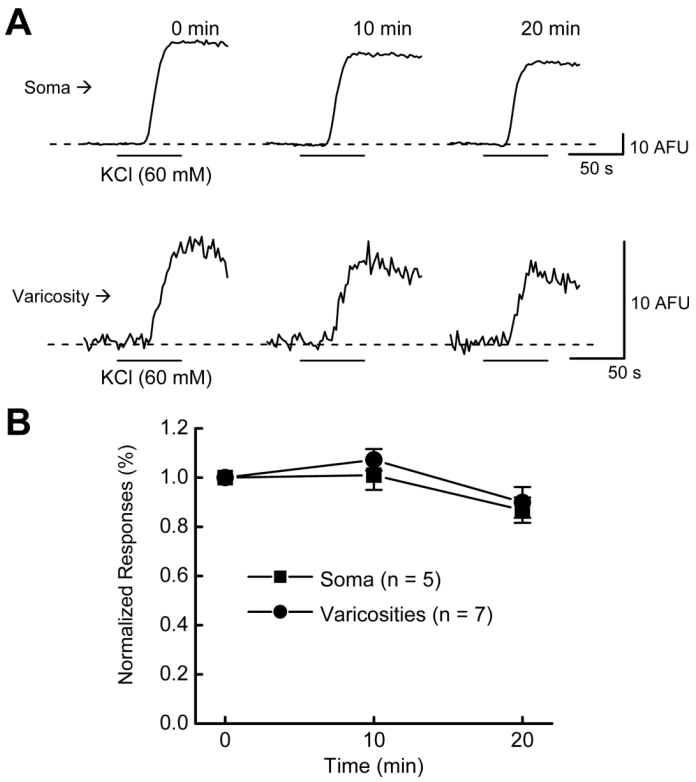

Figure 8.

Time control study for stability of $\Delta[Ca^{2+}]_i$ during 3 successive KCl (60 mM) applications. Data are $\Delta[Ca^{2+}]_i$ caused by KCl depolarization at 10 minute intervals. Data were normalized to the first $\Delta[Ca^{2+}]_i$ response and are mean + s.e.m. $\Delta[Ca^{2+}]_i$ did not decline significantly over the time course of this protocol ($P > 0.05$).

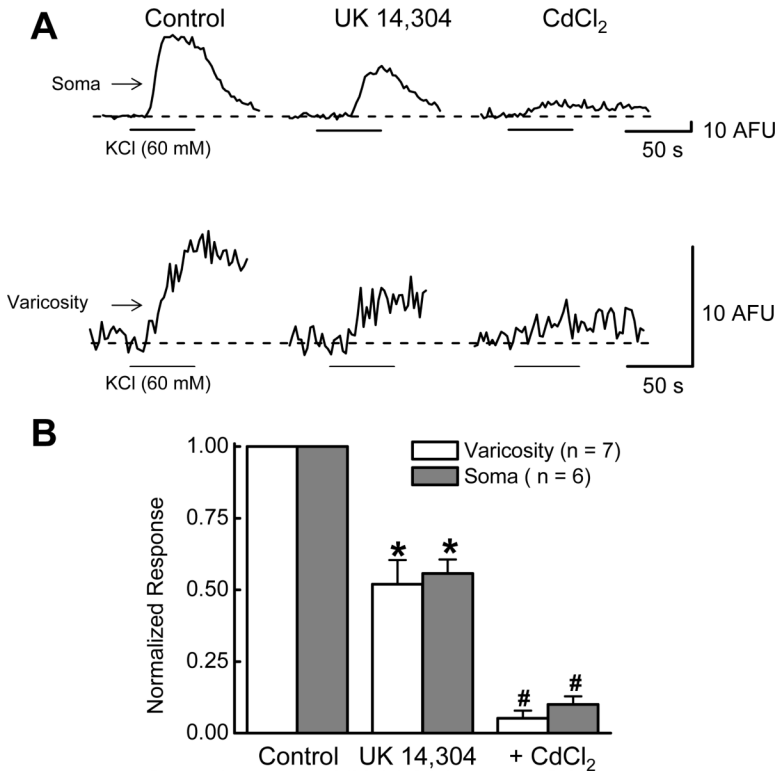

Figure 9.

Inhibitory effect of UK 14,304 on $\Delta[Ca^{2+}]_i$. A, Recordings $\Delta[Ca^{2+}]_i$ before and during application of KCl (60 mM) in the absence and presence of UK 14,304 (1 μM) and $CdCl_2$ (100 μM). UK 14,304 reduced $\Delta[Ca^{2+}]_i$ in both soma (upper traces) and a varicosity (lower traces). $\Delta[Ca^{2+}]_i$ evoked by KCl depolarization was blocked $CdCl_2$. B, Pooled data from experiments similar to that shown in "A". Control measurements made in individual soma or varicosities were set to a value of "1" and data obtained in the presence of UK 14,304 or $CdCl_2$ were expressed as a fraction of that control value. Data are mean ± s.e.m. *indicates significantly different from Control ($P < 0.05$). #indicates significantly different from measurements made in the presence of UK 14,304 ($P < 0.05$).

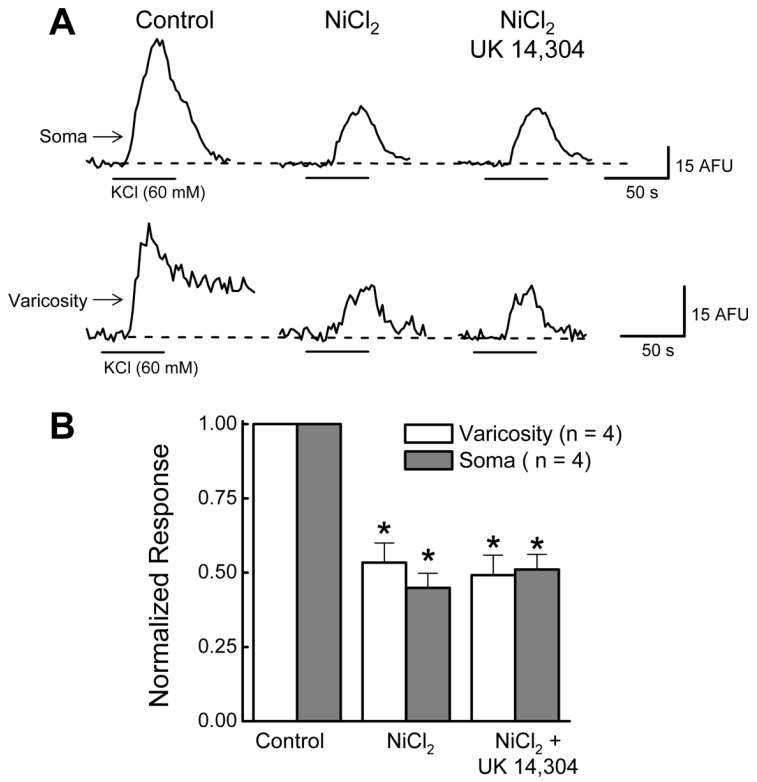

Figure 10.

UK 14,304 does not inhibit on $\Delta[Ca^{2+}]_i$ in the presence of $NiCl_2$ in soma and varicosities. A, Original recordings of $\Delta[Ca^{2+}]_i$ evoked by KCl (60 mM). $NiCl_2$ (50 μM) inhibited $\Delta[Ca^{2+}]_i$ in the soma (upper tracings) and varicosities (lower traces). Subsequent application of UK 14,304 (1 μM) did not alter $\Delta[Ca^{2+}]_i$ evoked by KCl depolarization. B, Pooled from experiments illustrated in "A". $NiCl_2$ inhibited $\Delta[Ca^{2+}]_i$ evoked by KCl in the soma and in varicosities while subsequent addition of UK 14,304 did not further reduce $\Delta[Ca^{2+}]_i$ evoked by KCl depolarization. Control measurements made in individual soma or varicosities were set to a value of "1" and data obtained in the presence of UK 14,304 or $NiCl_2$ were expressed as a fraction of that control value. Data are mean ± s.e.m. *indicates significantly different from Control ($P < 0.05$).

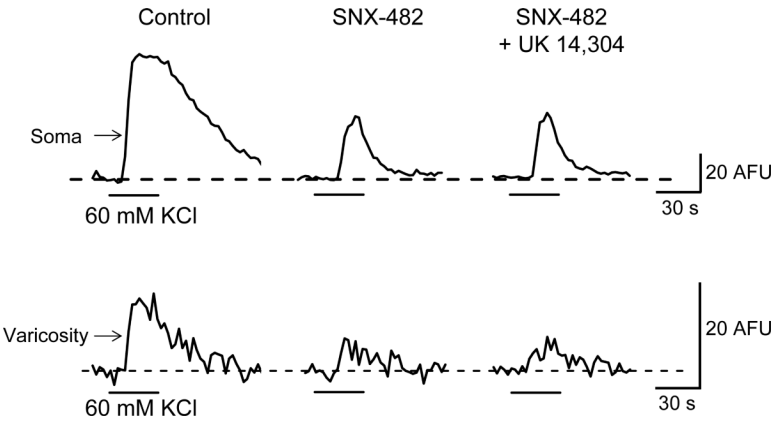

Figure 11.

UK 14,304 does not inhibit on $\Delta[Ca^{2+}]_i$ in the presence of SNX-482 in soma and varicosities. Original recordings of $\Delta[Ca^{2+}]_i$ evoked by 60 mM KCl. SNX-482 (0.1 μM) inhibited $\Delta[Ca^{2+}]_i$ in a soma (upper traces) and a varicosity (lower traces). Further application of UK 14,304 (1 μM) did not alter $\Delta[Ca^{2+}]_i$ evoked by KCl depolarization.